Effect of Local Heating on the Mechanical Characteristics of Repaired Automotive Panels

NICOLAE NAVODARIU[1], MIHAI BRANZEI[1]*, ROBERT CIOCOIU[1], ION CIUCA[1], RAZVAN COMAN[1], ANCA D. RAICIU[2], AUGUSTIN SEMENESCU[1], IULIAN ANTONIAC[1], SEBASTIAN GRADINARU[3]*, IOAN CRISTESCU[4]

[1]University Politehnica of Bucharest, 313 Splaiul Independentei Str., 060042, Bucharest, Romania

[2]Titu Maiorescu University, Faculty Pharmacy, Dept. Pharmacognosy Phytochem Phytoterapy, 16 Gh. Sincai Str., Bucharest, Romania

[3]Carol Davila University of Medicine and Farmacy, 37 Dionisie Lupu Str., 030167, Bucharest, Romania

[4] Clinical Emergency Hospital Bucharest, Department Orthoped & Traumatol, 8 Floreasca Av., 014461, Bucharest, Romania

Flame straightening is a technology process used to eliminate deformations. This method relies on local heating of the material to correct geometry or damaged parts. In the local automobile services its main use is for repairs of less critical deformed components. The maximum temperature and thermal gradient, heating time, cooling rate and number of heating cycles affect the mechanical properties since local heating can alter material microstructure. The aim of this research was to determine the mechanical characteristics of thin steel plates repaired by local heating associated with plastic deformation (similar to hot working) and cold straightening (similar to local cold working) for automotive side and door panels made of structural steel. Thin sheet plates, 0.9mm thickness, were deformed by impact and repaired by local heating using the flame and induction heating then plastically deformed while hot as well as straightened without heating. The heat repaired samples were studied by light microscopy to determine microstructure change and samples were tensile tested to determine their mechanical characteristics. Local excessive grain growth generates anisotropy, the assembly behaves as a composite material with regions that show significant plastic deformations while others little or no deformations at al. Without procedures adjusted to each material repairs involving heating are to be avoided, cold working should be employed when replacement is not possible.

Keywords: flame straightening, grain growth, mechanical characteristics

Flame straightening is a technology process used to eliminate deformations, usually in welded structures. Its principle relies on metallic materials behavior: their expansion when heated and contraction when cooled. If expansion is restricted compressive stresses are generated and upon their build up, the elastic limit of the material is superseded and the metallic material deforms plastically [1-3].

This common practice is applied for structural steels and can be applied to repair damaged elements and correct the geometry. By applying a heat source on the region of interest a thermal gradient appears: the region least heated, furthest from the heat source, restrains the deformation of the heated material and creates compressive stresses in the regions with high temperatures.

In practice, for product thickness less than 25mm an oxy-acetylene flame is used [4].

When flame straightened following parameters affect the mechanical properties of the material:

- maximum temperature;
- temperature gradient;
- heating time and cooling rate;
- the number of heating cycles.

The mechanical properties of the material are in direct relation with its microstructure, thus all parameters above need to be strictly controlled [5, 6].

In local automobile services flame straightening is used to repair components deformed in a car crash. Two heating methods are frequently employed: flame and induction. Regardless of the method employed, the process parameters are barely controlled: temperature is somewhat appreciated by color in a subjective manner, while heating pattern, time, number of cycles and cooling are disregarded.

The repaired components might be esthetically satisfactory but safety is greatly affected by the change of the mechanical characteristics of the repaired panel caused by grain growth and other microstructure changes when heating is involved [4-6].

**email: mihai.branzei@upb.ro; gradinarusebastian@gmail.com*

All authors have participated equally in developing this study.

The aspect of repaired components needs to be accounted for in the safety and crash performance of automotives and this research sets a base for further studies regarding these aspects.

Experimental part

Materials and methods

Two panels made of structural steel for the automotive industry were used for this study. The panels had prior deformations generated in a car crash. Repair procedures for mild impact imply local heating, local heating and deformation (similar to hot working) and cold working, depending on the damage degree.

Local heating was applied using two methods: using oxy-acetylene torch and induction heating in the region where the panel was deformed and local straightening was performed by slight hammering the deformed panels until satisfactory results were obtained. The local heated specimens were obtained in two states: heated and heated and deformed by slight bending into shape.

Sample coding and repair procedure applied is presented in table 1.

Table 1
SAMPLE CODING AND REPAIR PROCEDURES

Sample designation	Repair procedure applied
SP0	Reference sample, no repairs.
SPF	Local heating using oxy-acetylene torch.
SPFR	Local heating using oxy-acetylene torch + slight bending into shape.
SPI	Local heating using an inductor.
SPIR	Local heating using an inductor+ slight bending into shape.
SPCR	Repair by cold working.

The reference samples SP0 were obtained from replacement panels with no damage made of same structural steel.

Tensile specimens with dimensions according to ISO 6892-1 were then obtained from all panels, 3 samples/repair procedure, as described schematically in fig. 1.

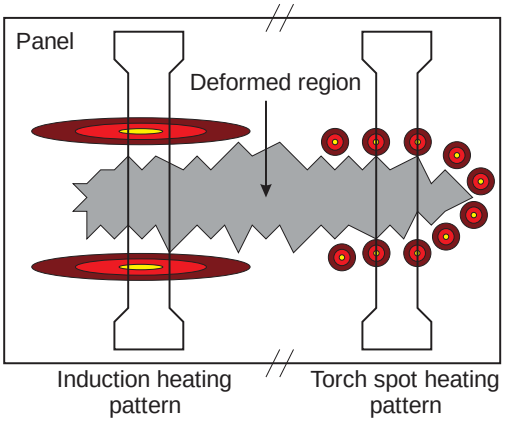

Fig. 1 Heating patterns for torch and induction means and tensile test sample specimen position

The samples were tested using a Walter+Bai servo-hydraulic universal testing machine in tension and ISO 6892-1 procedures applied to determine mechanical characteristics.

From the heated specimens metallographic specimens were obtained and prepared accordingly for light microscopy studies and using the Reichert Univar microscope and its bundled software package.

The chemical composition of the steel was determined using the Spectromaxx optic emission spectrometer.

Results and discussions

The chemical composition of the steel was determined on each panel used in this study by optical emission spectrometry. In table 1 an average chemical composition is presented.

Table 1
CHEMICAL COMPOSITION OF THE STEEL

Element	%C	%Si	%Mn	%Cr	%Ni	%Cu	%P	%S	%Fe
%wt	0.054	0.062	0.114	0.027	0.024	0.012	0.016	0.0096	Bal.

This chemical composition is generic and found in most standards as structural non alloy mild steel complying to steels with Werkstoffnummer 1.0389 and 1.0335 which specify carbon content less than 0.08% and manganese content less than 0.45%. The phosphorus and sulfur contents fall below the half of the specification, 0.025% and 0.030%.

For metallographic observations the samples were cut, mounted and prepared following the specific procedure for steels. Grain size measurement was performed using a Heyn lineal intercept procedure using an array of 20 vertical and horizontal lines, in fig. 2 horizontal line placement is shown on the different regions of microstructure.

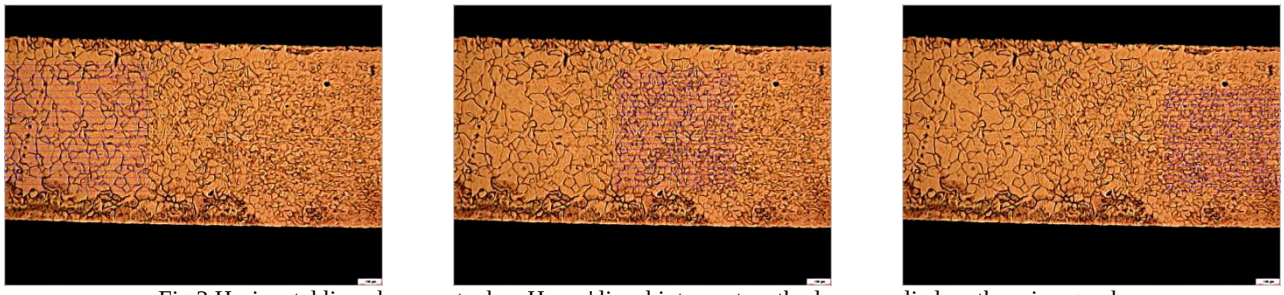

Fig.2 Horizontal line placement when Heyns' lineal intercept method was applied on the micrograph

In fig. 3 the grain size number G is shown for the various regions of microstructure. The value G is a mediated value from the results on vertical and horizontal results.

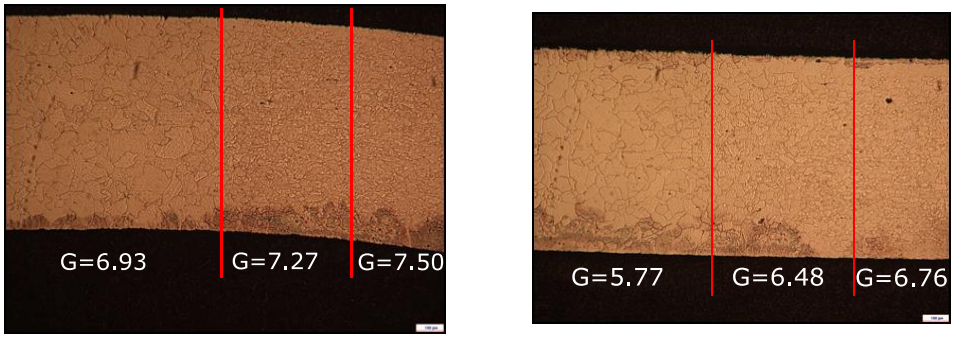

a. b.

Fig. 3 Microstructure of the steel showing local heating effects on microstructure and grain size when a. oxy-acetylene torch and b. induction heating was used

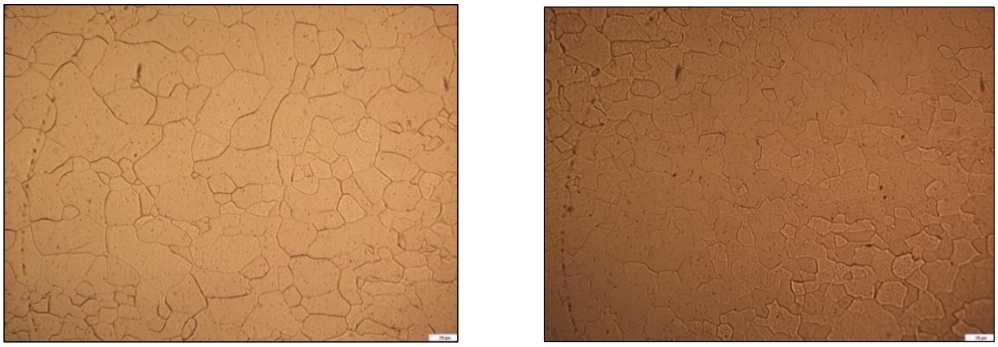

Fig. 4 Microstructure of the steel from an as delivered panel

The microstructures presented in fig. 3 are obtained in a transverse section relative to the long axis of the panel. It can clearly be seen how local heating generates an excessive grain growth in the heated region and next to it heat influences are clearly observable on grain size. By induction heating grain growth was more pronounced when compared to oxy-acetylene torch method.

The nominal grain size of the steel determined on an unaltered specimen was G=10.39.

The normal microstructure of the steel, shown in fig. 4, is formed of feritic grains with a slight preferred orientation given by cold working.

The tensile specimens were tested on the universal testing machine according to ISO 6892-1 specifications. A stress - strain comparison is shown in fig. 3 a, while in fig. 3.b details from the yield point region are shown. The specimens that were not heated showed no apparent yielding, while heated specimens do, as seen in fig. 5.b for specimen SPFR, SPF and SPIR.

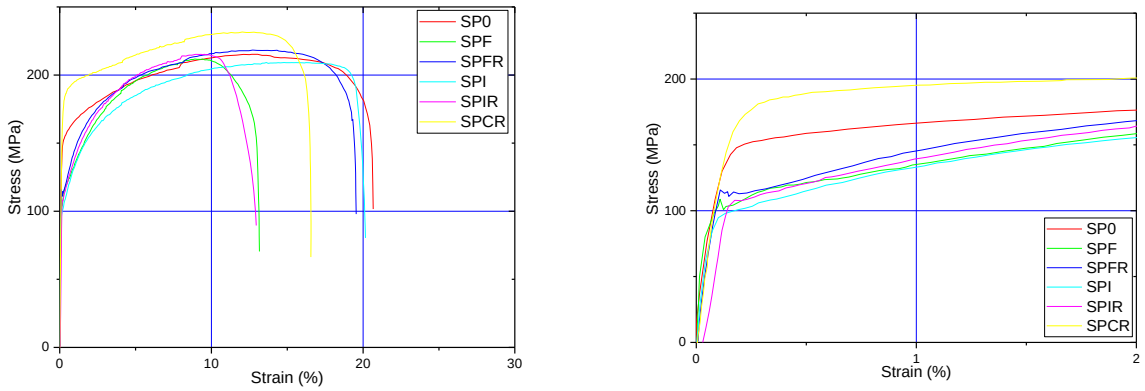

a. b.

Fig. 5 Stress - strain curves for the tested specimens showing a. general overview and b. a detail on the yield point region of the curve

The apparent yield point is specific for steels in an annealed state, thus local heating caused phase transformation in the material similar to those in an annealing heat treatment [7-10]. The stress-strain curve of the sample repaired by cold working resembles the one of the reference, thus the steel was cold worked with a certain degree when shaped for the panel.

The sample heated by induction SPI did not manifest an apparent yield point and our conclusion is inconstant heating in the repair procedure. In workshop conditions temperature is appreciated by heating colors which are subjective and strongly influenced by ambient lighting.

In fig. 6 to 11 the bar charts show the comparisons of the mechanical characteristics determined post stress - strain curve processing.

In fig. 6 the tensile strength was highest for the reference sample SP0 and second the cold worked sample SPCR. The heated samples SPF and SPI have the lower values, induction heating resulted in the lowest tensile strength. Slight bending during heating results in an increase in tensile strength values.

The yield strength variation shown in fig. 7 is according to expectations: by cold working an increase is expected, as shown by sample SPCR, and, when heated - similar to an annealing, a drop in yield strength was observed. Slight bending on the heated samples did not create a significant increase in yield strength value.

Comparing the percentage plastic extension at maximum force in fig. 8 an unexpected result was observed: the cold worked sample SPCR showed largest extension, followed closely by the induction heated sample SPI. Same variation was observed for the percentage total extension at maximum force in fig. 9.

The percentage elongation after fracture variation shown in fig. 8 and the percentage total extension at maximum fracture shown in fig. 10 are similar. Largest extension appears in the cold worked sample SPCR, while the lowest value is to be observed in the flame heated and bent sample SPFR. The largest extensions in the cold worked sample, SPCR, are a consequence of remnant deformed regions which straightened when the test sample was stressed.

According to theory by cold working the mechanical characteristics (hardness, tensile strength) are to increase, while plasticity (quantified by extensions) are to decrease. When annealed, the reverse is expected: plasticity is expected to increase and mechanical characteristics are to decrease.

The results from the tests do not agree to the theory given the local heating of test samples followed by microstructure changes which results in a "composite" material behavior [11-13].

The behavior of the tensile specimens was studied by the slope change on the load-displacement curves where uniform plastic deformation occurs. The load-displacement curve was segmented into three regions where the variation was almost linear and the slope and the intercept determined in a manner similar to a spring constant or the stiffness of a body, details are shown in fig. 12.

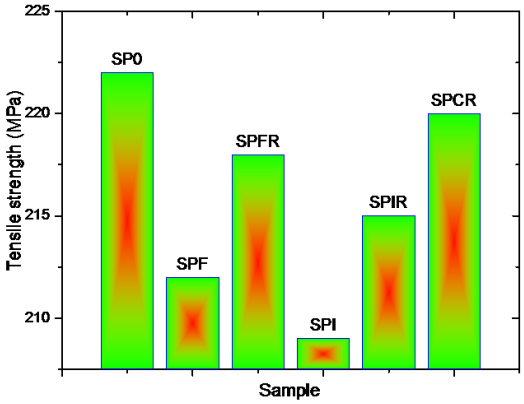

Fig. 6 Tensile strength comparison

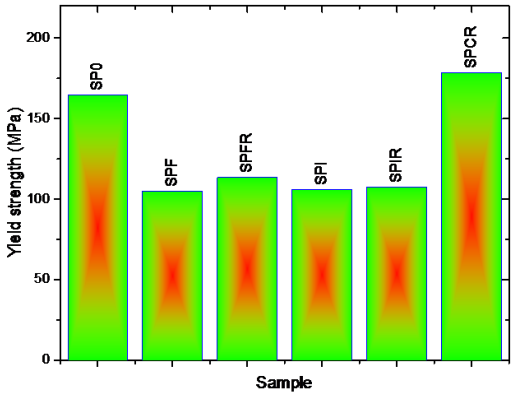

Fig. 7 Yield strength comparison

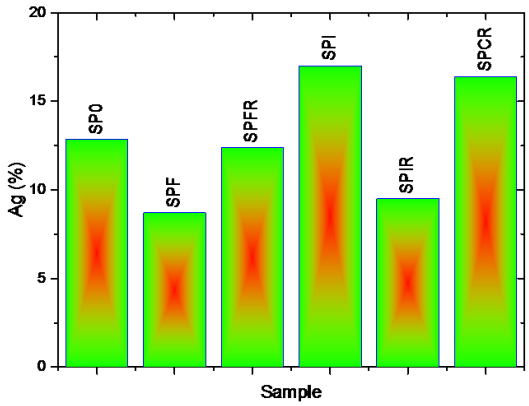

Fig. 8 Percentage plastic extension at maximum force comparison

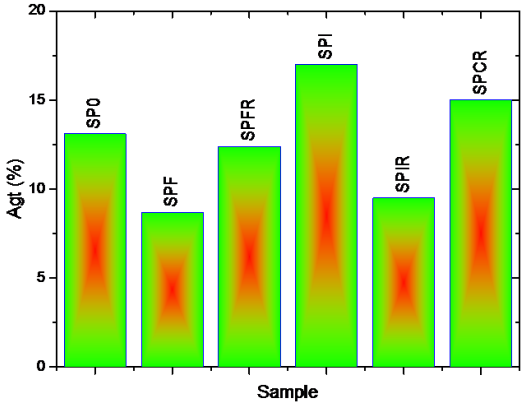

Fig. 9 Percentage total extension at maximum force comparison

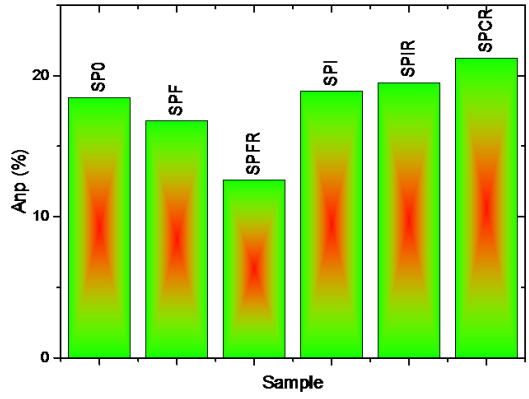

Fig. 10 Percentage elongation after fracture comparison

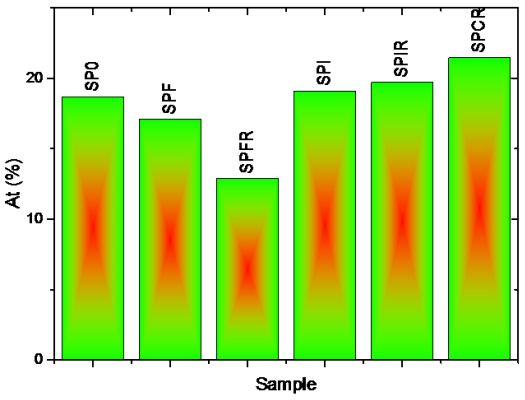

Fig. 11 Percentage total extension at maximum fracture comparison

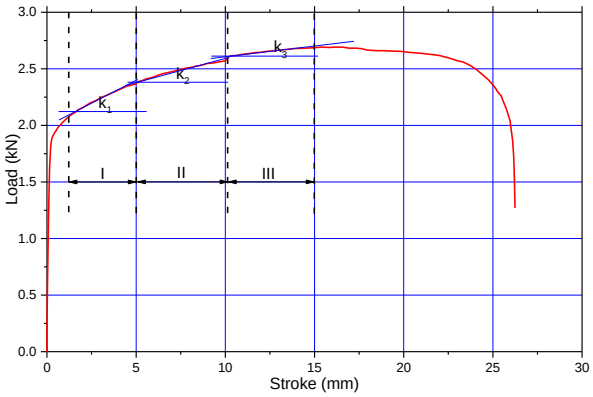

Fig. 12 Processing of the load - displacement curve by segmenting into three regions with linear behavior and slope estimation

On each region 5 points were randomly selected and a linear regression was fitted in order to determine the slope and the intercept, as shown in fig. 13.

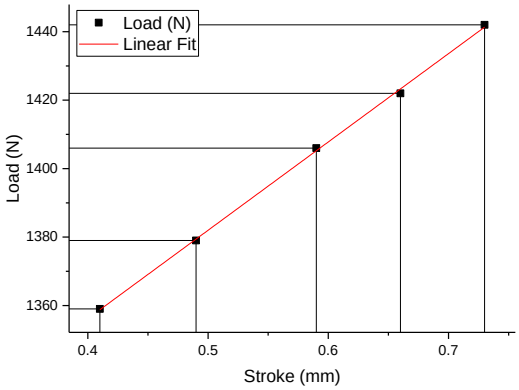

Fig. 13. Linear fit on a set of five random selected points

The estimated slopes k_1, k_2 and k_3 and corresponding intercepts i_1, i_2 and i_3 are presented in table 2.

Table 2
ESTIMATED SLOPES AND INTERCEPTS

Sample	k_1 [N/mm]	i_1 [N]	k_2 [N/mm]	i_2 [N]	k_3 [N/mm]	i_3 [N]
SP0	62.86	1897.56	27.39	2082.10	4.40	2371.70
SPF	258.07	1252.95	44.75	2017.63	7.29	2388.84
SPFR	260.12	1244.03	30.77	1965.51	2.50	2320.63
SPI	373.93	1056.42	62.24	1666.48	4.64	2249.49
SPIR	328.79	1105.17	39.15	1925.04	11.44	2200.47
SPCR	46.71	1957.16	30.74	2040.88	5.14	2353.87

The behavior in the first region of the curve described by k_1 reflects that the samples heated by induction require highest energy to deform the material and same observation can apply to the samples heated using the torch. The reference and cold repaired samples are on another magnitude level, the slope values are about 6 times lower than those heated by induction. This could be caused by microstructure change caused by a thermal treatment similar to a recrystallization annealing or normalizing in the heated samples, while the other samples are already plastically deformed.

In the second region, where k_2 is used as descriptor for the behavior, it can be seen that all samples fall in the same range of values while and in the third region according to k_3 the samples behave in the same manner.

The intercept value shows same variation as the yield strength which it was to be expected and it was not considered a valuable descriptor for the specimen behavior in tension.

In such structure the mechanical characteristics are decisive in stress and strain distribution. To illustrate the importance of such variation a finite element analysis was developed and performed in SolidWorks Simulation using a simplified model of the current case: an assembly was devised with 4 components with various mechanical characteristics adjusted to conform the experiment.

The assembly was stressed in tension and the results are presented in fig. 10.

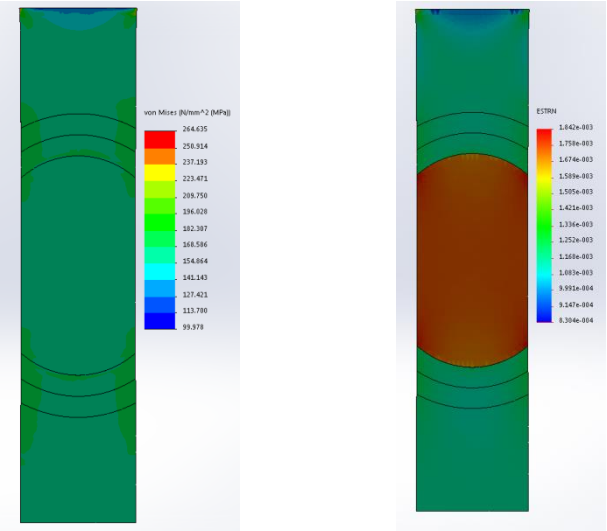

a. b.

Fig. 14 Simulation results showing a. von Misses stress and b. strain distribution in the assembly

The von Misses stresses are almost uniformly distributed in the specimen, as observed in fig. 14.a while the strain distribution presented in fig. 14.b suggests that the most strained region is in the center, where mechanical characteristics were parameterized as lowest. The uneven strain distribution can be a cause for the abnormal behavior of the specimens during the tensile tests].

The assembly can be modeled as a set of springs in series with different spring constants k_1 and k_2 as shown in fig. 15. The load F is uniformly distributed in the assembly as equation (1) states, while the equivalent extension x_{eq} is given by the summation of individual springs elongation x_1 and x_2 (2). Using the relations from equation (1) in equation (2) the equivalent spring constant k_{eq} can be determined using equation (3) and simplifying the force yields equation (4). The total elongation of the assembly is dictated by individual characteristics of the components and the spring with lowest mechanical characteristics is to deform strongest [14-16].

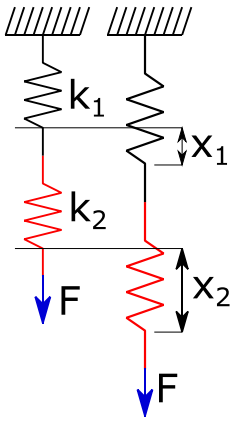

$$F = k_{eq} \cdot x_{eq} = k_1 \cdot x_1 = k_2 \cdot x_2 \quad (1)$$

$$x_{eq} = x_1 + x_2 \quad (2)$$

$$\frac{F}{k_{eq}} = \frac{F}{k_1} + \frac{F}{k_2} \quad (3)$$

$$\frac{1}{k_{eq}} = \frac{1}{k_1} + \frac{1}{k_2} \quad (4)$$

Fig. 15 The behavior of springs in series

The local deformations of the tensile test samples were studied by tracing a grid before testing and measuring the local deformations for each part. Both local elongation and narrowing were determined by dividing the change in length to its original length and multiplying the ratio by 100, the procedure is illustrated by fig. 16.

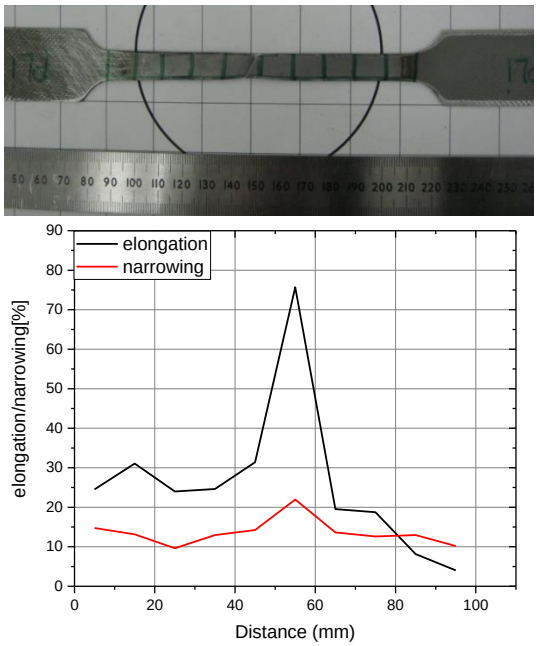

Fig.16 Tensile tested specimen with measuring grid with elongation and narrowing variation on the length of the specimen

The procedure described above was applied to each tested specimen and the local deformation is presented in fig. 17.

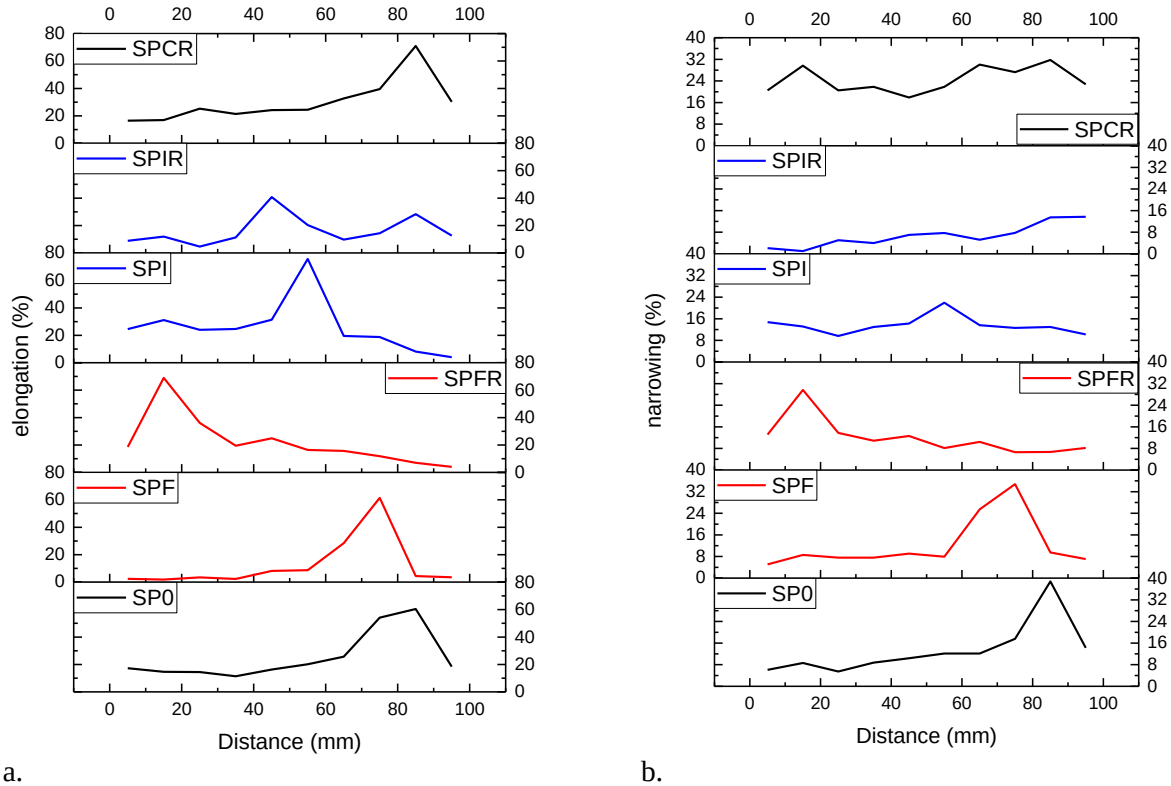

a. b.

Fig. 17 Deformations determined on the length of the test samples, a. showing local elongation and b. narrowing variations

The local elongations presented in fig. 17.a show that the reference sample SP0 and the one repaired by cold working, SPCR, show a gradual increase in elongation values peaking in the region where necking occurred, while the heated specimens show highly localized elongations, where repairs were performed.

The local narrowing shown in fig. 17.b resembles mostly the same variation of the elongations, the cold repaired sample SPCR shows an abnormal variation which can be regarded as a consequence of extremely localized strong deformations caused by hammer blows.

Conclusions

This study was destined to investigate how common repairs of deformed automotive panels affect structural integrity of the component. The results show that local heating, regardless of the method employed, causes local excessive grain growth with deleterious effects on mechanical characteristics and plasticity.

Induction heating, without proper control, caused most unfavorable structure in the material.

As descriptors for the mechanical performance the yield strength of the material is the most useful since it reflects the affected regions true characteristics.

The repaired panel becomes anisotropic, the heated regions deform strongest and become fracture initiation sites.

The procedures involving heating need to be optimized and material dependent parameters set to obtain good results.

Repairs performed without heating offered best results and when panel replacement is not possible this is the procedure recommended.

References

1. CULLISON, A., Weld J 1995, 74, 12-12
2. VACKAR, B. K., DOLIDA, R. J., Weld J 1981, 60, 25-27
3. HUBO, R.; KUGLER, D.; PETERSEN, J.; WEGMANN, H., Stahl Eisen 1994, 114, 97-&
4. ZHAO, D. S., HUANG, Z. Y., MIAO, T. J., Destech Trans Mat 2016, 33-38
5. CAI, C. W., WANG, X., LIANG, Z. M., RAO, Y. Z., WANG, H. B., YAN, D. J., Metals-Basel 2018, 8
6. ANTONIAC I., SINESCU C., ANTONIAC A., J Adhes Sci Technol., 30(16), 2016, p. 1711-1715.
7. POPESCU M., PUIU D., RAICIU A.D., Rev Chim. (Bucharest), **69**, no. 9, 2018, p.2338-2342
8. RAICIU A.D., POPESCU M., MANEA S., et al., Rev Chim. (Bucharest), **67**, no. 10, 2016, p.1936-1939.
9. GHEORGHE, D., POP, D., et al., U.P.B. Sci. Bull., Series B, 81 (1), 2019, 244-258
10. ONODERA, R., HE, Z. G., MORITA, I., J Jpn I Met 2002, 66, 521-527
11. CHITEA, C., TOMOAIA, G., TOADER, O.D., MILEA, C., TRANTE, O., EARAR, K., SACELEANU, V., Rev Chim. (Bucharest), **70**, no. 4, 2019, 1460-1465
12. BOLCU, D., STANESCU, M. M., CIUCA, I., TRANTE, O., MIHAI, B., Mat. Plat., 46, 2009, p. 206-210
13. STANESCU, M. M., BOLCU, D., CIUCA, I., RIZESCU, S., TRANTE, O., BAYER, M., Mat. Plast., **47**, 2010, p. 103-108
14. GRECU D., ANTONIAC I., TRANTE O. et al., Mat. Plast., **53**, no. 4, 2016, p.776-780.
15. ANTONIAC, I.V., STOIA D.I., GHIBAN B., TECU C., MICULESCU F., VIGARU C., SACELEANU V., Materials. 2019; 12(7):1128
16. POUYA, M., WINTER, S., FRITSCH, S., WAGNER, M. F. X.,19th Chemnitz Seminar on Materials Engineering 2017, 181.
17. VILCIOIU, J. D.; ZAMFIRESCU, D. G.; CRISTESCU, I.; URSACHE, A.; POPESCU, S. A.; CREANGA, C. A.; LASCAR, I., Rom J Morphol Embryo 2016, **57**, 567-572.
18. TECU, C.; ANTONIAC, I.; GOLLER, G.; YAVAS, B.; GHEORGHE, D.; ANTONIAC, A.; CIUCA, I.; SEMENESCU, A.; RAICIU, A. D.; CRISTESCU, I., Mat. Plast, **56**, 2019, p. 644-648.
19. MOLDOVAN, M.; BALAZSI, R.; SOANCA, A.; ROMAN, A.; SAROSI, C.; PRODAN, D.; VLASSA, M.; COJOCARU, I.; SACELEANU, V.; CRISTESCU, I., Materials 2019, **12**.
20. PAUN, M. A.; FRUNZA, A.; STANCIULESCU, E. L.; MUNTEANU, T. C.; CRISTESCU, I.; GRAMA, S.; CHIOTOROIU, A.; ENE, A.; MIHAI, C., Ind Textila 2019, **70**, 242-247.

Manuscript received: 20.11.2019